PHYSICAL REVIEW A VOLUME 16, NUMBER 3 SEPTEMBER 1977

K-shell x rays of selected elements from Nb through Gd for incident protons and alpha particles from 0.6 to 2.4 MeV

S. R. Wilson, F. D. McDaniel, J. R. Rowe, and J. L. Duggan
Department of Physics, North Texas State University, Denton, Texas 76203*
(Received 28 February 1977)

K-shell x-ray production cross sections and $K\beta/K\alpha$ ratios are presented for 0.6- to 2.4-MeV protons and alpha particles incident on thin targets of selected elements from Nb to Gd. The $K\beta/K\alpha$ ratios are compared to the theoretical predictions of Scofield and agree within 10%. The experimental cross sections are compared to the theoretical predictions of the plane-wave Born approximation (PWBA) and the PWBA modified to include binding energy, Coulomb deflection, and relativistic effects. It is seen that the PWBA modified for binding energy and Coulomb deflection effects agrees with the experimental data for Nb to within uncertainties, but its predictions are lower than the data by larger amounts as the target Z increases. Inclusion of an *ad hoc* semiclassical relativistic correction to the theoretical cross section, as suggested by Hansen, improves the agreement with the data, but overestimates the data for the highest-Z elements.

I. INTRODUCTION

In the past few years there has been considerable interest in inner-shell ionization produced in light-ion–atom collisions. Earlier experimental data have been summarized in review articles by Rutledge and Watson[1] and by Garcia, Fortner, and Kavanagh.[2] These results have been compared primarily to two theoretical models of Coulomb ionization: (a) the binary-encounter approximation[3] (BEA) and (b) the plane-wave Born approximation (PWBA). The present data are outside the range of values tabulated by McGuire and Richard[4] for the BEA, and therefore the BEA theory will not be compared to the data.

The PWBA developed by Merzbacher and Lewis[5] has been found to be in good agreement with experimental cross sections for incident projectiles of atomic mass ≤ 4 and for energies greater than a few MeV.[6,7] However, at lower incident projectile energies, the PWBA overpredicts the cross sections.[6,8] The PWBA has been modified by Basbas, Brandt, and Laubert[9,10] to include Coulomb deflection of the incident ion by the target nucleus and increased binding of the target electron due to penetration of the K shell by the projectile. Both of these modifications, which are important at lower incident velocities, reduce the theoretical cross sections and improve agreement with experiment.[8]

Relativistic effects which are believed to be important particularly at low incident ion velocities for heavier targets are expected to increase the theoretical cross sections.[11-16] For targets with high Z_2, the crucial relativistic effect has its origin in the singularity of the K-shell wave function at the origin. This increases the form factor for the large values of momentum transfer which are needed for ionization by projectiles with low velocities. The enhancement of the form factor increases the cross section at low velocities and the effect subsides as velocity increases. Merzbacher and Lewis[5] have noted that the apparent agreement between K-shell cross sections of uranium for proton bombardment and the nonrelativistic PWBA is coincidental and is most likely due to a cancellation of the effects of increased binding energy and Coulomb deflection with relativistic effects. Merzbacher and Lewis[5] discuss a relativistic correction due to Hönl.[12] Recently, Caruso and Cesati[13] have also modified the PWBA to include relativistic effects. Both of these corrections[12,13] modify the target screening parameter θ_K and do not depend on the incident particle's velocity. Hansen[14] has suggested a semiclassical relativistic correction for the BEA, and this correction has been applied in an *ad hoc* manner to the PWBA in the present work. This correction consists of a multiplicative factor applied to the nonrelativistic theoretical cross section and depends on the ratio of the incident particle velocity squared to the average target K-shell electron velocity squared.

The majority of K-shell x-ray production cross-section data reported for 0.5–3.0-MeV proton[17-26] and α-particle[8,27-29] bombardment are for elements in the range of Z_2 from 20 to 40. Gray and co-workers[21,23] have reported proton-induced cross sections for selected elements between $_{42}$Mo and $_{57}$La. Liebert *et al.*[26] reported proton data for $_{42}$Mo, $_{47}$Ag, and $_{48}$Cd. McKnight, Thornton, and Karlowicz[27] present data for α particles on $_{42}$Mo, $_{47}$Ag, and $_{50}$Sn. Lin, Duggan, and Carlton[28] have presented data for α particles on $_{47}$Ag.

Absolute cross sections for elements in the range of $Z_2 = 40-65$ are needed to provide a test

of relativistic corrections to the PWBA since relativistic effects are expected to be large for protons and α particles incident on heavy elements at energies less than a few MeV. These cross sections should also be quite useful to the many laboratories involved in particle-induced x-ray emission studies of trace elements.[30]

K-shell x-ray production cross sections and $K\beta/K\alpha$ ratios are measured in this work for 0.6–2.4-MeV protons incident on thin targets of $_{41}$Nb, $_{45}$Rh, $_{47}$Ag, $_{49}$In, $_{53}$I, $_{55}$Cs, $_{58}$Ce, $_{59}$Pr, $_{60}$Nd, $_{63}$Eu, and $_{64}$Gd. Also presented are data for α particles incident on $_{41}$Nb, $_{42}$Mo, $_{45}$Rh, $_{47}$Ag, $_{50}$Sn, $_{51}$Sb, $_{53}$I, $_{56}$Ba, $_{58}$Ce, and $_{64}$Gd. The $K\beta/K\alpha$ ratios are compared to the theoretical predictions of Scofield [31] and the experimental values compiled by Salem *et al.*[32] The cross-section data are compared to the theoretical predictions of the PWBA with and without modifications for increased binding, Coulomb deflection,[9,10] and relativistic effects.[14]

II. EXPERIMENTAL PROCEDURE

The targets used in this experiment were from 3 to 136 μg/cm^2 thick, and are listed in Table I. The targets were made from vacuum evaporation of the element or compound of the element on carbon backings. The backings, which had been mounted on Al frames, ranged in thickness from 25 to 50 μg/cm^2.

The proton and α-particle beams were produced by the 2.5-MV Van de Graaff accelerator at North Texas State University. The beam was collimated to 2 mm in diameter before entering the target chamber which is shown in Fig. 1. The transmission targets were mounted at 45° with respect to the incident beam direction, and the x-ray detector was positioned inside the scattering chamber

TABLE I. Experimental target thicknesses.

Target	Thickness (μg/cm^2)
$_{41}$Nb	3.24
$_{42}$Mo	3.00
$_{45}$Rh	8.70
$_{47}$Ag	53.0
$_{49}$In	133
$_{50}$Sn	86.0
$_{51}$Sb	11.7
$_{53}$I	26.6
$_{55}$Cs	136
$_{56}$Ba	50.2
$_{58}$Ce	96.5
$_{59}$Pr	39.1
$_{60}$Nd	31.5
$_{63}$Eu	15.9
$_{64}$Gd	12.1

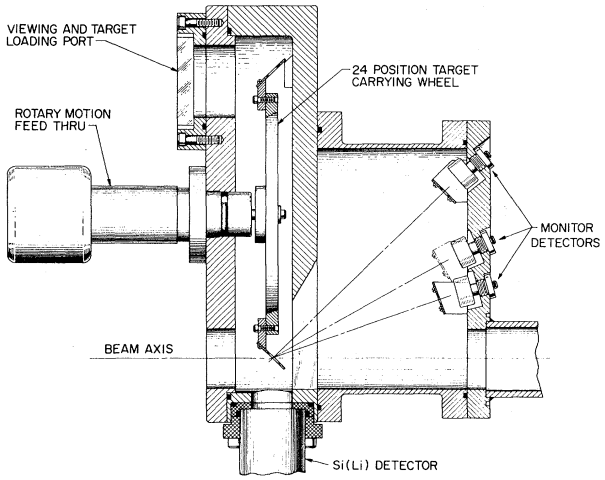

FIG. 1. Atomic foil wheel scattering chamber.

at 90° with respect to the incident beam direction. Two x-ray detectors were used in this work: (i) an Ortec Si(Li) detector with a full width at half maximum (FWHM) resolution of 165 eV at 5.9 keV and (ii) an Ortec intrinsic Ge detector with a FWHM resolution of 237 eV at 5.9 keV and 511 eV at 122 keV. Both detectors were calibrated for energy and efficiency by placing calibrated x-ray sources of ^{57}Co, ^{65}Zn, ^{155}Eu, and ^{241}Am in the target position. These point sources simulated the actual geometry of x-ray emission from the targets due to ion bombardment. This method of calibration is widely used and has been discussed in the literature.[33] The total efficiencies for both detectors are shown in Fig. 2 as a function of x-ray energy. The efficiencies include contributions from the intrinsic detector efficiencies and the detector solid angles. The solid angles subtended by the Si(Li) and Ge detectors were 1.2×10^{-2} and 8.2×10^{-2} sr, respectively. The solid lines represent least-squares polynomial fits to the efficiencies over the regions of interest for the present work. Mylar foils of thickness 0.036 and 0.061 cm were placed over the Si(Li) and Ge detector windows, respectively, and were used to attenuate low-energy x rays. The Si(Li) spectrometer was used to detect the characteristic x rays of $_{41}$Nb, $_{42}$Mo, $_{45}$Rh, $_{47}$Ag, $_{49}$In, and $_{55}$Cs. The x rays from $_{47}$Ag, $_{49}$In, $_{50}$Sn, $_{51}$Sb, $_{53}$I, $_{56}$Ba, $_{58}$Ce, $_{59}$Pr, $_{60}$Nd, $_{63}$Eu, and $_{64}$Gd were detected using the Ge detector because of its higher efficiency for x rays of these energies. Both detectors were used in measurements for protons on $_{49}$In and α particles on $_{47}$Ag. Results obtained for $_{49}$In and $_{47}$Ag using the two different detectors were found to agree within 10%. A Si surface-barrier detector, located at an angle

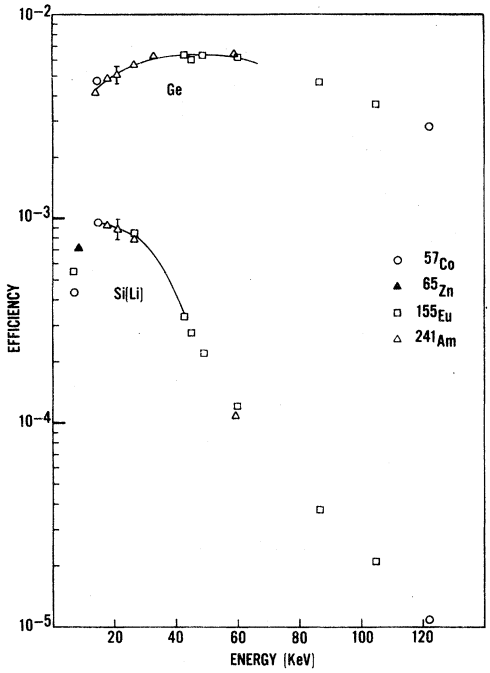

FIG. 2. Experimentally determined detector efficiencies.

of 150° with respect to the incident beam direction and with a solid angle of 8.1×10^{-4} sr, was used to detect incident particles that were Rutherford scattered by the target atoms.

Charged-particle and x-ray energy spectra were recorded simultaneously in a Nuclear Data multichannel analyzer in order to limit problems in target uniformity. Consequently, the absolute x-ray cross sections could be determined by normalizing to Rutherford scattered ions, as discussed earlier.[34] Corrections for beam energy loss in the target as suggested by Laubert *et al.*[35] were <4% for proton data and generally ≤10% for α-particle data. Beam currents were constantly adjusted to keep the particle and x-ray dead time to 5% or less.

III. RESULTS AND DISCUSSION

The measured values of the proton-induced K x-ray production cross sections and the $K\beta/K\alpha$ intensity ratios for the various elements are presented in Table II. Table III presents the α-particle-induced x-ray production cross sections and $K\beta/K\alpha$ ratios. The proton-induced x-ray production cross sections for $_{47}$Ag determined in this work were compared to the results of Khelil and Gray,[23] Bearse *et al*,[18] and Bissinger, Shafroth, and Waltner.[19] Results agreed to within 10% or better at energies greater than 1.0 MeV and to within 20% or better at energies ≤1.0 MeV. Bearse *et al.*[18] reported only $K\alpha$ x-ray production cross sections, and it was necessary to multiply these numbers by $1+K\beta/K\alpha$ in order to compare their values with the present work. McKnight, Thornton, and Karlowicz[27] have reported ionization cross sections for α particles incident on $_{42}$Mo, $_{47}$Ag, and $_{50}$Sn. For comparison with the present measurements, their data have been multiplied by the fluorescence yields for single-hole ionization taken from Bambynek *et al.*[36] Their data for $_{42}$Mo agree to within a few percent with the measurements of the present work. Their results[27] for $_{47}$Ag and $_{50}$Sn were lower than the present measurements by 50–65%. In light of the disagreements for $_{47}$Ag and $_{50}$Sn, the cross sections for incident 2-MeV α particles were remeasured in our laboratory and were found to be in agreement with the previous NTSU measurements to within 5% for $_{47}$Ag and to within 13% for $_{50}$Sn.

Figure 3 presents the measured proton-induced x-ray cross sections for $_{41}$Nb, $_{45}$Rh, $_{47}$Ag, $_{49}$In, $_{53}$I, $_{55}$Cs, $_{58}$Ce, $_{59}$Pr, $_{60}$Nd, $_{63}$Eu, and $_{64}$Gd. α-particle-induced x-ray cross sections for $_{41}$Nb, $_{42}$Mo, $_{45}$Rh, $_{47}$Ag, $_{50}$Sn, $_{51}$Sb, $_{53}$I, $_{56}$Ba, $_{58}$Ce, and $_{64}$Gd are shown in Fig. 4. The smooth lines through the data merely serve to guide the eye. These two figures show the characteristic decrease in cross section with increasing atomic number of the target and the increase in cross section with increasing projectile energy. It is noted that the cross section for the lightest element, $_{41}$Nb, and that for the heaviest element, $_{64}$Gd, differ by over two orders of magnitude for the same projectile at the same energy.

The experimental x-ray production cross sections for representative elements of $_{41}$Nb and $_{64}$Gd are compared to the theoretical K-shell cross sections in Figs. 5 and 6, respectively, using fitted values of the fluorescence yields for single-hole ionization taken from Bambynek *et al.*[36] The data are compared to the plane-wave Born approximation (PWBA)[5,9,37]; the PWBA modified for increased binding (PWBA-B)[9]; the PWBA modified for Coulomb deflection (PWBA-C)[9]; the PWBA modified for both increased binding and Coulomb deflection (PWBA-BC)[9]; and the PWBA modified for increased binding, Coulomb deflection, and relativistic effects[14] (PWBA-BCR). Basbas, Brandt, and Laubert[10] have suggested a further modification to the PWBA-BC to account for the target polarization at higher velocities. This effect is not considered here because it changes the theory by less than 1% for the measurements of this work.

The uncertainties shown in Figs. 5 and 6 are relative uncertainties only, and come from quantities which vary with energy. These relative uncertainties are due mainly to statistics and vary from 5 to 20%. Normalization uncertainties, those

TABLE II. Proton-induced K-x-ray production cross sections[a] and $K\beta/K\alpha$ ratios.[b]

Energy (MeV)	Protons σ_X (b)	$K\beta/K\alpha$
	$_{41}$Nb	
1.13	3.6±0.4(−1)	0.15
1.34	6.5±0.6(−1)	0.18
1.55	1.0±0.1	0.17
1.76	1.6±0.1	0.18
1.97	2.1±0.2	0.19
2.18	3.0±0.3	0.19
2.39	3.6±0.3	0.19
2.60	4.5±0.4	0.17
2.70	4.8±0.4	0.19
	$_{45}$Rh	
1.03	1.0±0.1(−1)	0.19
1.24	2.1±0.2(−1)	0.22
1.45	3.4±0.3(−1)	0.19
1.66	5.2±0.4(−1)	0.20
1.87	7.7±0.6(−1)	0.20
2.07	1.1±0.1	0.18
2.29	1.5±0.1	0.22
2.50	1.9±0.2	0.18
2.70	2.2±0.2	0.19
	$_{47}$Ag	
0.4	9.0±1.0(−4)	0.20
0.6	9.4±0.8(−3)	0.23
0.8	3.3±0.3(−2)	0.21
1.0	7.9±0.6(−2)	0.22
1.2	1.4±0.1(−1)	0.21
1.4	2.3±0.2(−1)	0.21
1.6	3.6±0.3(−1)	0.22
1.8	5.2±0.4(−1)	0.21
2.0	7.5±0.6(−1)	0.22
2.2	9.9±0.8(−1)	0.22
2.4	1.3±0.1	0.21
	$_{49}$In	
0.6	5.5±0.4(−3)	0.22
0.8	1.9±0.2(−2)	0.22
1.0	5.0±0.4(−2)	0.23
1.2	8.5±0.7(−2)	0.22
1.4	1.5±0.1(−1)	0.22
1.6	2.3±0.2(−1)	0.22
1.8	3.5±0.3(−1)	0.22
2.0	5.0±0.4(−1)	0.22
2.2	6.6±0.5(−1)	0.23
2.4	8.5±0.6(−1)	0.22
	$_{53}$I	
0.6	1.5±0.2(−3)	0.29
0.8	6.2±0.5(−3)	0.26
1.0	1.4±0.1(−2)	0.24
1.2	3.2±0.3(−2)	0.23
1.4	5.9±0.5(−2)	0.22
	$_{53}$I	
1.6	9.2±0.7(−2)	0.22
1.8	1.5±0.1(−1)	0.24
2.0	2.1±0.2(−1)	0.24
2.2	3.0±0.3(−1)	0.24
2.4	3.6±0.3(−1)	0.22
	$_{55}$Cs	
1.13	1.6±0.2(−2)	0.16
1.34	2.8±0.2(−2)	0.23
1.55	5.0±0.4(−2)	0.24
1.76	7.8±0.6(−2)	0.26
1.97	1.1±0.1(−1)	0.22
2.18	1.7±0.1(−1)	0.24
2.39	2.1±0.2(−1)	0.22
2.60	2.9±0.2(−1)	0.26
2.70	3.0±0.2(−1)	0.24
	$_{58}$Ce	
0.6	3.2±0.3(−4)	0.28
0.8	1.7±0.1(−3)	0.23
1.0	5.1±0.4(−3)	0.27
1.2	1.1±0.1(−2)	0.25
1.4	2.1±0.2(−2)	0.25
1.6	3.1±0.2(−2)	0.25
1.8	5.6±0.4(−2)	0.26
2.0	7.4±0.6(−2)	0.25
2.2	1.1±0.1(−1)	0.26
2.4	1.4±0.1(−1)	0.23
	$_{59}$Pr	
0.6	2.9±0.3(−4)	0.30
0.8	1.3±0.1(−3)	0.28
1.0	3.7±0.3(−3)	0.27
1.2	8.3±0.7(−3)	0.25
1.4	1.6±0.1(−2)	0.24
1.6	2.7±0.2(−2)	0.25
1.8	3.9±0.3(−2)	0.25
2.0	5.7±0.4(−2)	0.27
2.2	8.1±0.6(−2)	0.25
2.4	1.0±0.1(−1)	0.25
	$_{60}$Nd	
0.6	2.1±0.3(−4)	0.25
0.8	1.1±0.1(−3)	0.23
1.0	3.4±0.3(−3)	0.28
1.2	8.1±0.7(−3)	0.27
1.4	1.6±0.1(−2)	0.28
1.6	2.6±0.2(−2)	0.27
1.8	3.9±0.3(−2)	0.25
2.0	5.3±0.4(−2)	0.28
2.2	7.5±0.6(−2)	0.25
2.4	9.7±0.8(−2)	0.26

TABLE II. (*Continued*)

Energy (MeV)	Protons σ_X(b)	$K\beta/K\alpha$	Energy (MeV)	Protons σ_X (b)	$K\beta/K\alpha$
	$_{63}$Eu			$_{64}$Gd	
0.8	8.5±0.8(–4)	0.30	0.8	7.1±0.7(–4)	0.29
1.0	2.0±0.2(–3)	0.27	1.0	2.2±0.2(–3)	0.28
1.2	4.5±0.4(–3)	0.28	1.2	4.9±0.4(–3)	0.27
1.4	9.1±0.8(–3)	0.25	1.4	8.6±0.7(–3)	0.29
1.6	1.4±0.1(–2)	0.29	1.6	1.5±0.1(–2)	0.27
1.8	2.3±0.2(–2)	0.26	1.8	2.1±0.2(–2)	0.28
2.0	3.3±0.3(–2)	0.28	2.0	3.3±0.3(–2)	0.28
2.2	4.4±0.4(–2)	0.27	2.2	4.4±0.3(–2)	0.28
2.4	5.9±0.5(–2)	0.29	2.4	5.6±0.5(–2)	0.27

[a] The notation (–N) associated with the cross section means $\times 10^{-N}$.
[b] All $K\beta/K\alpha$ uncertainties are less than 10%.

which do not change with energy, are due primarily to efficiency and solid angle uncertainties and vary from 5 to 15%. The uncertainties listed in Tables II and III are total uncertainties found from the square root of the sum of the squares of the relative and normalization uncertainties, and range from 7 to 24%. The sources of uncertainty in the measured cross sections have been discussed earlier.[8]

All of the theories presented in Fig. 5 tend to predict the general shape of the experimental data for the lightest element studied, $_{41}$Nb. The PWBA modified for both binding energy and Coulomb deflection (PWBA-BC) agrees with the proton-induced cross sections for $_{41}$Nb to within experimental uncertainties. However, the PWBA-BC predicts cross sections lower than the α-particle data by 65% at the low energies and 45% at the

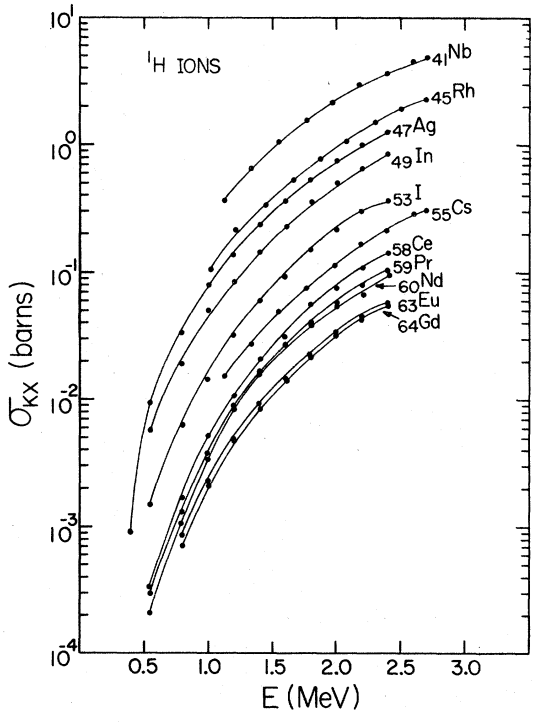

FIG. 3. Experimental proton-induced x-ray production cross sections for the elements studied in this work.

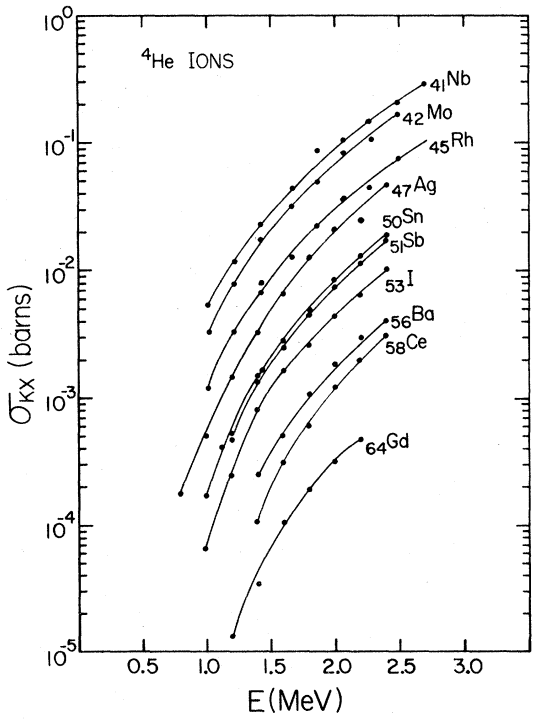

FIG. 4. Experimental K-shell x-ray production cross sections for α particles incident on the elements studied in this work.

TABLE III. α-particle-induced K-x-ray production cross sections[a] and $K\beta/K\alpha$ ratios.[b]

Energy (MeV)	α particles σ_X (b)	$K\beta/K\alpha$	Energy (MeV)	α particles σ_X (b)	$K\beta/K\alpha$
	$_{41}$Nb			$_{51}$Sb	
1.02	5.4 ± 0.8(−3)	0.23	1.2	4.7 ± 0.9(−4)	0.21
1.23	1.1 ± 0.2(−2)	0.20	1.4	1.3 ± 0.2(−3)	0.21
1.44	2.3 ± 0.2(−2)	0.20	1.6	2.5 ± 0.3(−3)	0.22
1.66	4.3 ± 0.4(−2)	0.20	1.8	4.6 ± 0.5(−3)	0.21
1.87	8.5 ± 0.7(−2)	0.19	2.0	7.3 ± 0.7(−3)	0.22
2.08	1.0 ± 0.1(−1)	0.18	2.2	1.2 ± 0.1(−2)	0.20
2.29	1.4 ± 0.1(−1)	0.18	2.4	1.7 ± 0.2(−2)	0.20
2.49	2.0 ± 0.2(−1)	0.16			
2.70	2.8 ± 0.2(−1)	0.20			
	$_{42}$Mo			$_{53}$I	
1.02	3.3 ± 0.5(−3)	0.21	1.0	6.6 ± 0.7(−5)	
1.23	8.0 ± 0.9(−3)	0.21	1.2	2.5 ± 0.2(−4)	0.25
1.44	1.7 ± 0.2(−2)	0.18	1.4	8.1 ± 0.9(−4)	0.24
1.66	3.1 ± 0.3(−2)	0.19	1.6	1.7 ± 0.2(−3)	0.22
1.87	4.9 ± 0.5(−2)	0.17	1.8	2.6 ± 0.3(−3)	0.23
2.08	7.8 ± 0.8(−2)	0.16	2.0	4.3 ± 0.4(−3)	0.23
2.29	1.1 ± 0.1(−1)	0.15	2.2	6.5 ± 0.6(−3)	0.25
2.49	1.6 ± 0.2(−1)	0.17	2.4	1.0 ± 0.1(−2)	0.22
	$_{45}$Rh				
1.02	1.2 ± 0.2(−3)	0.21			
1.23	3.3 ± 0.4(−3)	0.18		$_{56}$Ba	
1.44	6.6 ± 0.7(−3)	0.18	1.4	2.5 ± 0.6(−4)	
1.66	1.3 ± 0.1(−2)	0.21	1.6	5.0 ± 0.7(−4)	0.21
1.87	2.2 ± 0.2(−2)	0.19	1.8	1.0 ± 0.2(−3)	0.23
2.08	3.7 ± 0.4(−2)	0.16	2.0	1.8 ± 0.3(−3)	0.26
2.29	4.5 ± 0.4(−2)	0.23	2.2	3.0 ± 0.4(−3)	0.22
2.49	7.4 ± 0.6(−2)	0.19	2.4	4.9 ± 0.6(−3)	0.22
2.70	9.9 ± 0.7(−2)	0.20			
	$_{47}$Ag				
0.8	2.1 ± 0.3(−4)	0.21		$_{58}$Ce	
1.0	5.4 ± 0.6(−4)	0.22	1.4	1.1 ± 0.2(−4)	
1.2	1.5 ± 0.1(−3)	0.22	1.6	3.1 ± 0.7(−4)	0.23
1.4	3.6 ± 0.3(−3)	0.23	1.8	5.9 ± 1.0(−4)	0.21
1.6	6.3 ± 0.6(−3)	0.23	2.0	1.2 ± 0.1(−3)	0.23
1.8	1.2 ± 0.1(−2)	0.21	2.2	2.0 ± 0.4(−3)	0.22
2.0	2.0 ± 0.2(−2)	0.21	2.4	3.0 ± 0.6(−3)	0.24
2.2	2.6 ± 0.2(−2)	0.24			
2.4	4.3 ± 0.4(−2)	0.22			
	$_{50}$Sn				
1.0	1.7 ± 0.3(−4)	0.23			
1.2	5.3 ± 0.6(−4)	0.22		$_{64}$Gd	
1.4	1.5 ± 0.1(−3)	0.22	1.2	1.3 ± 0.2(−5)	
1.6	2.8 ± 0.3(−3)	0.19	1.4	4.4 ± 0.7(−5)	0.29
1.8	4.6 ± 0.4(−3)	0.21	1.6	1.0 ± 0.1(−4)	0.27
2.0	8.5 ± 0.8(−3)	0.20	1.8	1.9 ± 0.3(−4)	0.26
2.2	1.3 ± 0.1(−2)	0.20	2.0	3.1 ± 0.4(−4)	0.26
2.4	1.9 ± 0.2(−2)	0.19	2.2	4.7 ± 0.5(−4)	0.28

[a] The notation $(-N)$ associated with the cross sections means $\times 10^{-N}$.
[b] All $K\beta/K\alpha$ uncertainties are less than 10%.

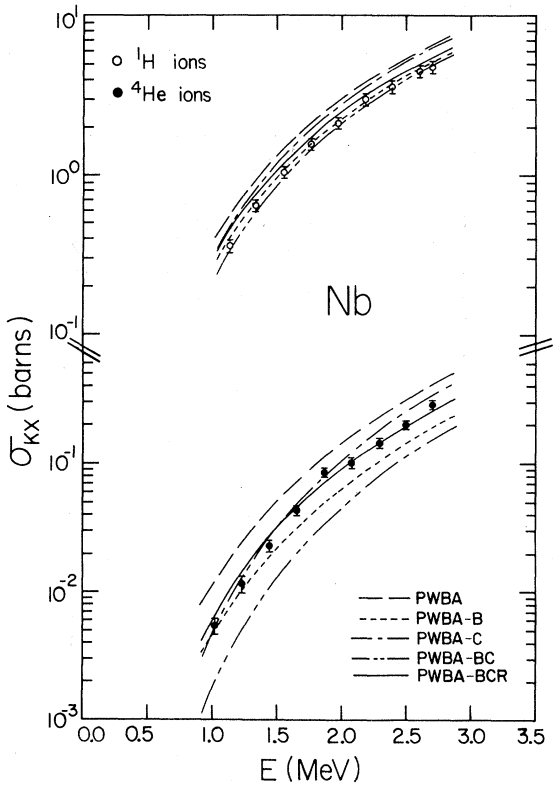

FIG. 5. K-shell x-ray production cross sections for protons and α particles incident on $_{41}$Nb. The experimental data are compared to the plane-wave Born approximation (PWBA) with modifications for increased binding (B), Coulomb deflection (C), and relativistic effects (R).

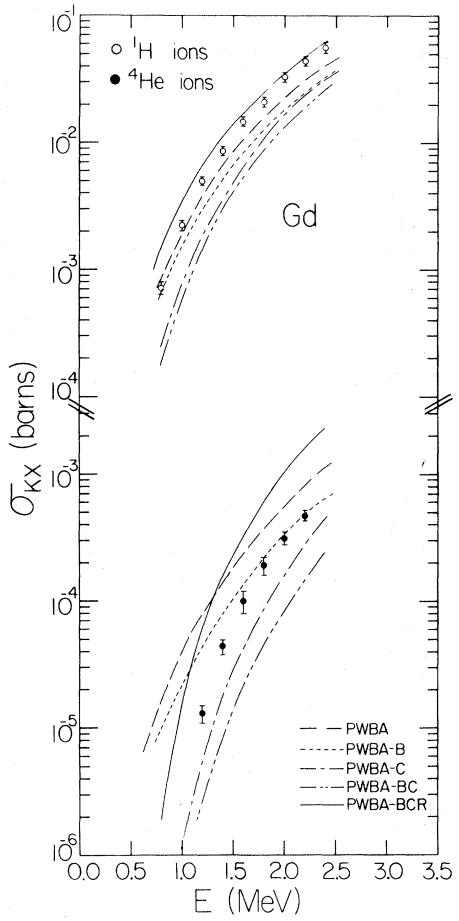

FIG. 6. K-shell x-ray production cross sections for protons and α particles incident on $_{64}$Gd. The experimental data are compared to the plane-wave Born approximation (PWBA) with modifications for increased binding (B), Coulomb deflection (C), and relativistic effects (R).

high energies. Multiplying the PWBA-BC by the relativistic correction suggested by Hansen[14] raises the theoretical cross section and improves the agreement with the data.

Figure 6 compares the experimental data for proton and α particles incident on $_{64}$Gd, the heaviest element studied. For protons and α particles on $_{64}$Gd, the PWBA-BC predicts values less than the data at all energies by factors of 2–3 with the disagreement becoming larger at lower projectile velocities. The relativistic correction raises the PWBA-BC and gives better agreement with the proton data especially above 2 MeV. For proton energies less than 2 MeV, the relativistic correction appears to be too large and causes the PWBA-BCR to be almost a factor of 2 larger than the data at 0.8 MeV. For α particles on Gd, the relativistic correction is again too large and causes the PWBA-BCR to overestimate the data by a factor of 4.5–5 at all energies. This may be because the values of the relativistic corrections have not been calculated exactly, but are extrapolated from the table by Hansen.[14] In some cases, the extrapolated correction raised the theory by more than an order of magnitude.

It was seen in Figs. 5 and 6 that even for the PWBA-BCR the theoretical calculations deviate from the data as the ratios of incident ion velocity to K-shell electron velocity decreases. This can easily be seen if the data are put in the form of a universal plot as described earlier.[34] If the ionization process is accurately described by the PWBA formalism, the measured cross sections should exhibit a universal behavior for all values of the variable η_K and θ_K when scaled by the Coulomb deflection correction ($9E_{10}$), the fluorescence yield (ω_0), the relativistic correction[14] (R), and ($\sigma_{0K}/\epsilon\theta_K$). In this formalism,[9] η_K is the reduced particle-velocity parameter; θ_K is the reduced binding energy; and ϵ is the binding-energy correction.

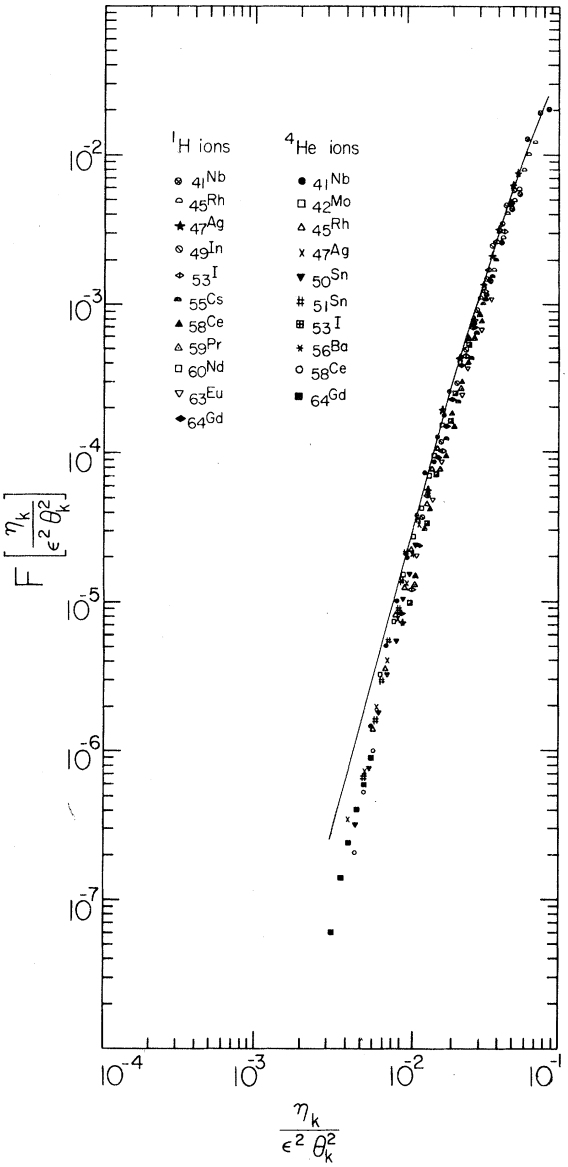

FIG. 7. Experimental proton and α-particle-induced x-ray production cross sections scaled as a function of $\eta_K/\epsilon^2\theta_K^2$ for comparison to the approximate universal function $F(\eta_K/\epsilon^2\theta_K^2)$ in the PWBA theory of Basbas *et al.* (Ref. 9).

An experimentally inferred universal function, F^{expt}, is given by[34]

$$F\left(\frac{\eta_K}{\epsilon^2\theta_K^2}\right)^{\text{expt}} = \frac{\sigma_{KX}^{\text{expt}}}{R\omega_0 9E_{10}(b\epsilon\theta_K\eta_K^{-3/2})(\sigma_{OK}/\epsilon\theta_K)},$$

and the reduced data are presented in Fig. 7. The solid line in Fig. 7 is the theoretical universal function $F(\eta_K/\epsilon^2\theta_K^2)$ which has been tabulated by Basbas, Brandt, and Laubert[9] and Khandelwal, Choi, and Merzbacher,[38] and was calculated for

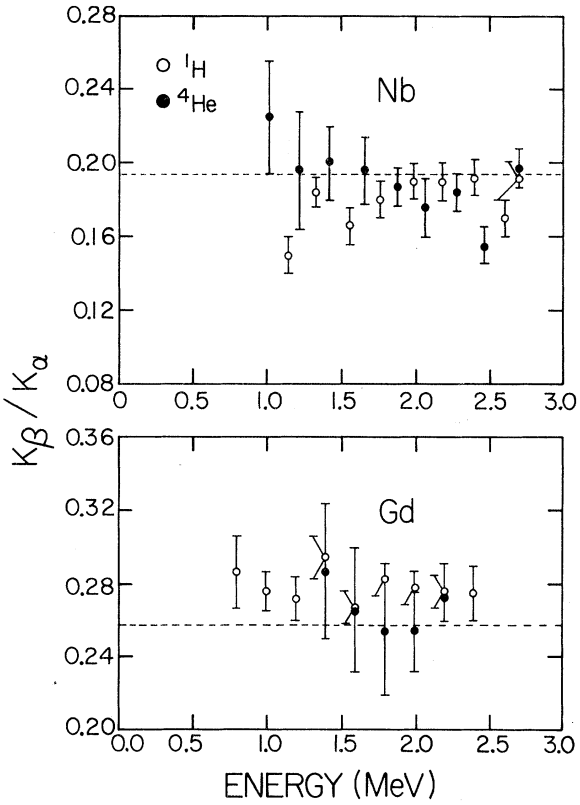

FIG. 8. Proton and α-particle-induced $K\beta/K\alpha$ ratios for $_{41}$Nb and $_{64}$Gd. The dashed lines are the theoretical predictions of Scofield (Ref. 31). Note suppressed zero.

the present work using an analytical expression given by Brandt and Lapicki.[37] The theory predicts the data to within a few percent for values of $\eta_K/(\epsilon\theta_K)^2$ greater than 4×10^{-2}. However, for values less than this, the theory's predictions begin to overestimate the data by as much as a factor of 4.5. This is because the relativistic correction[14] is too large for this range of $\eta_K/(\epsilon\theta_K)^2$.

$K\beta/K\alpha$ ratios for Nb and Gd are shown in Fig. 8. The apparent constancy of the $K\beta/K\alpha$ ratio indicates very little multiple ionization for these projectile-target combinations at these energies. The dashed lines are the theoretical prediction of Scofield.[31] Because the average proton-induced $K\beta/K\alpha$ ratios were above the theoretical predictions[31] for Gd by 8%, the ratio was measured using

TABLE IV. $K\alpha_2/K\alpha_1$ ratios.

Element	Experimental $K\alpha_2/K\alpha_1$	Theoretical[a] $K\alpha_2/K\alpha_1$
$_{63}$Eu	0.553 ± 0.027	0.554
$_{64}$Gd	0.555 ± 0.028	0.556

[a]Reference 31.

a ^{155}Eu source which undergoes β decay to Gd and emits Gd x rays due to internal conversion. The measured source ratio was also high, but only by 3%. The $K\alpha_2/K\alpha_1$ ratios were measured for Eu and Gd at the higher proton energies. The averaged results are presented in Table IV and agree with the value of Scofield[31] to within 1%.

In conclusion, it was seen that $K\beta/K\alpha$ ratios, for protons and α particles incident on the high-Z (41–64) elements studied in this work, agree with the values of Scofield to better than 10%. The $K\alpha_2/K\alpha_1$ ratios for Eu and Gd agree with Scofield to within 1%. Although the PWBA modified for increased binding and Coulomb deflection agrees with the proton-induced x-ray cross sections for $_{41}$Nb within uncertainties, it underestimates the majority of the other data by larger amounts as the target Z increases. Inclusion of an *ad hoc* correction[14] to the theoretical cross sections for relativistic effects improves the agreement with the data, but overcorrects the theories for the highest-Z elements. A rigorous incorporation of relativistic effects into the PWBA formalism would do much toward developing a comprehensive model of light-ion induced inner-shell ionization.

ACKNOWLEDGMENTS

We would like to thank R. Rice, G. Monigold, W. Holland, F. Elliott, R. Mehta, L. Hawthorne, J. Tricomi, D. Ray, and D. Johnson for assistance in various aspects of data collection and analysis. We would like to thank J. H. McGuire and G. Basbas for helpful discussions concerning relativistic effects.

*Supported in part by the Robert A. Welch Foundation, the NTSU Faculty Research Fund, and the Research Corporation.

[1]C. H. Rutledge and R. L. Watson, At. Data Nucl. Data Tables 12, 195 (1973).
[2]J. D. Garcia, R. J. Fortner, and T. M. Kavanagh, Rev. Mod. Phys. 45, 111 (1973).
[3]J. D. Garcia, E. Gerjuoy, and J. E. Welker, Phys. Rev. 165, 66 (1968); J. D. Garcia, Phys. Rev. A 1, 1402 (1970); 1, 280 (1970).
[4]J. H. McGuire and P. Richard, Phys. Rev. A 8, 1374 (1973).
[5]E. Merzbacher and H. W. Lewis, *Handbuch der Physik*, edited by S. Flügge (Springer-Verlag, Berlin, 1958), Vol. 34, p. 166.
[6]W. Brandt, in *Proceedings of the International Conference on Inner-Shell Ionization Phenomena and Future Applications, Atlanta, Georgia, 1972*, edited by R. W. Fink, S. T. Manson, J. M. Palms, and P. V. Rao (U. S. AEC Report No. CONF-720404, Natl. Tech. Inform. Service, Oak Ridge, Tenn., 1972) p. 948.
[7]R. Akselsson and and T. B. Johansson, Z. Phys. 266, 245 (1974).
[8]F. D. McDaniel, T. J. Gray, and R. K. Gardner, Phys. Rev. A 11, 1607 (1975).
[9]G. Basbas, W. Brandt, and R. Laubert, Phys. Rev. A 7, 983 (1973).
[10]G. Basbas, W. Brandt, and R. Laubert, Bull. Am. Phys. Soc. 18, 103 (1973); and unpublished.
[11]D. Jamnik and C. Zupancic, K. Dan. Vidensk. Selsk. Mat.-Fys. Medd. 31, No. 2 (1957).
[12]H. Hönl, Z. Phys. 84, 1 (1933).
[13]E. Caruso and A. Cesati (unpublished).
[14]J. S. Hansen, Phys. Rev. A 8, 822 (1973).
[15]F. D. McDaniel, T. J. Gray, R. K. Gardner, G. M. Light, J. L. Duggan, H. A. Van Rinsvelt, R. D. Lear, G. H. Pepper, J. W. Nelson, and A. R. Zander, Phys. Rev. A 12, 1271 (1975).
[16]J. Tricomi, J. L. Duggan, F. D. McDaniel, P. D. Miller, R. P. Chaturvedi, R. M. Wheeler, J. Lin, K. A. Kuenhold, L. A. Rayburn, and S. J. Cipolla, Phys. Rev. A 15, 2269 (1977).
[17]G. A. Bissinger, J. M. Joyce, E. J. Ludwig, W. S. McEver, and S. M. Shafroth, Phys. Rev. A 1, 841 (1970).
[18]R. C. Bearse, D. A. Close, J. J. Malanify, and C. J. Umbarger, Phys. Rev. A 7, 1269 (1973).
[19]G. A. Bissinger, S. M. Shafroth, and W. A. Waltner, Phys. Rev. A 5, 2046 (1972).
[20]R. Lear and T. J. Gray, Phys. Rev. A 8, 2469 (1973).
[21]T. L. Criswell and T. J. Gray, Phys. Rev. A 10, 1145 (1974).
[22]J. F. Chemin, J. Roturier, B. Saboya, Q. T. Dien, and J. P. Thibaud, Phys. Rev. A 11, 549 (1975).
[23]N. A. Khelil and T. J. Gray, Phys. Rev. A 11, 893 (1975).
[24]W. N. Lennard and I. V. Mitchell, Phys. Rev. A 12, 1723 (1975).
[25]H. Tawara, Y. Hachiya, K. Ishii, and S. Morita, Phys. Rev. A 13, 572 (1976).
[26]R. B. Liebert, T. Zabel, D. Miljanic, H. Larson, V. Valkovic, and G. C. Phillips, Phys. Rev. A 8, 2336 (1973).
[27]R. H. McKnight, S. J. Thornton, and P. R. Karlowicz, Phys. Rev. A 9, 267 (1974); and private communications.
[28]J. Lin, J. L. Duggan, and R. F. Carlton, Ref. 6, p. 998.
[29]C. G. Soares, R. D. Lear, J. T. Sanders, and H. A. Van Rinsvelt, Phys. Rev. A 13, 953 (1976).
[30]S. A. E. Johansson and T. B. Johansson, Nucl. Instrum. Methods 137, 473 (1976).
[31]J. H. Scofield, Phys. Rev. A 9, 1041 (1974).
[32]S. I. Salem, S. L. Panossian, and R. A. Krause, At. Data Nucl. Data Tables 14, 91 (1974).
[33]L. B. Magnusson, Phys. Rev. 107, 161 (1957); R. J. Gehrke and R. A. Lokken, Nucl. Instrum. Methods 97, 219 (1971); J. S. Hansen, J. C. McGeorge, D. Nix, W. D. Schmidt-Ott, I. Unus, and R. W. Fink, Nucl. Instrum. Methods 106, 365 (1973); W. J. Gallagher and S. J. Cipolla, Nucl. Instrum. Methods 122, 405 (1974); J. L. Campbell and L. A. McNelles, Nucl. Instrum. Methods 117, 519 (1974); 125, 205 (1975).

[34]F. D. McDaniel, J. L. Duggan, P. D. Miller, and G. D. Alton, Phys. Rev. A 15, 846 (1977).
[35]R. Laubert, H. Hazelton, J. R. Mowat, R. S. Peterson, and I. A. Sellin, Phys. Rev. A 11, 135 (1975).
[36]W. Bambynek, B. Crasemann, R. W. Fink, H.-U. Freund, H. Mark, C. D. Swift, R. E. Price, and P. V. Rao, Rev. Mod. Phys. 44, 716 (1972).
[37]W. Brandt and G. Lapicki, Phys. Rev. A 10, 474 (1974).
[38]G. S. Khandelwal, B. H. Choi, and E. Merzbacher, At. Data 1, 103 (1969).